

Supplementary data

Material and Methods

Cell culture

Murine macrophage-like RAW264.7 cells (ATCC, TIB-71 strain), human embryonic kidney cell line HEK293T cells (ATCC, CRL-11268 strain), mouse primary macrophages and BMDM cells were cultured in DMEM medium (Cat. #C12430500BT, GIBCO, Thermofisher scientific, Waltham, MA) supplemented with 10% fetal bovine serum (FBS) (Cat. #10099141, GIBCO), 100 U/mL penicillin and 100 µg/mL streptomycin. Human primary monocytes were cultured in RPM1640 medium (Cat. #C11875500BT, GIBCO) supplemented with 10% FBS, 100 U/mL penicillin and 100 µg/mL streptomycin. Cells were incubated at 37°C in a humidified incubator with 5% CO₂.

BMDMs isolation

BMDM cells were isolated as we previously performed (1). Briefly, cells were isolated from mouse bone marrow and maintained in DMEM supplemented with 10% FBS and 30% L929 cell supernatant for 7 days. The purity of BMDM was identified as > 95% by flow cytometry.

Magnetic sorting of primary cells

Human CD14⁺ monocytes were sorted from peripheral blood mononuclear cells (PBMCs) by positive selection with Anti-human CD14 magnetic particles (Cat. #557769, BD Biosciences), as we previously performed (1). In brief, human PBMCs were isolated with Ficoll Separation Medium (Cat. #LTS1077-1, TBD, Tianjin, China). CD14⁺ monocytes were sorted with anti-human CD14 magnetic particles, which are magnetic nanoparticles with monoclonal CD14 antibody conjugated to their surfaces for the positive selection of CD14-bearing monocytes via BD IMag™ Cell Separation Magnet. Mouse peritoneal and splenic macrophages were sorted with EasySep™ Mouse F4/80

Positive Selection Kit (Cat. #100-0659) purchased from STEMCELL, which are magnetic nanoparticles with monoclonal F4/80 antibody to select F4/80-bearing macrophages. For splenic cell sorting, the whole spleen tissue was taken from sacrificed mice and washed twice in PBS to remove the remaining blood. Then the spleen was cut into small pieces with scissors and tweezers and put into the digestive solution containing 100 µg/ml Collagenase D (Sigma-Aldrich, St. Louis, MO, USA) and 10 µg/ml DNase I (Thermo Fisher Scientific, Waltham, MA, USA), shaking for 1 hour at 37 °C. After the digestion, cells were collected through a 70 µm cell filter and centrifuged at 1500 rpm. Finally, cells were treated with lysing buffer (BD, Catalog# 559759) to remove blood red cells and collected by centrifugation for further sorting. The status and purities of sorting cells were detected by flow cytometry (**Figure S19**).

Plasmid construction

Plasmids containing murine TREM2, SHP1, SHIP1, SHP2, PGC-1 α , PGC-1 β , Syk or BTK with an C-terminal tag were constructed. Full length genes were amplified by reverse transcription-PCR and cloned into PSG5 vector. C-SH2, N-SH2 and PTPase domains of SHP1 were cloned based on the full-length SHP1 plasmid. TREM2 plasmids deleting extracellular domain (Δ Extra) or transmembrane plus cytoplasmic domain (Δ Trans-cyto) were constructed on the basis of full-length TREM2 plasmid. R352A, K356 A, R358 A, N359 A, Y536 A and Y564 A mutants of SHP1 were generated with MultiS Fast Mutagenesis kit V2 (Cat. #C215-01, Vazyme, Nanjing, China) following the manufacturer's recommendations. All constructed plasmids were confirmed by sequencing and their expressions in 293T cells were detected by western blot with anti-Tag antibodies.

Cell transfection

Cells were transfected with negative control siRNA against TREM2 (siTREM2, Ribobio) or constructed plasmids using Lipofectamine 2000 (Cat. #11668019, Thermofisher) according to the manufacturer's instructions. 6 hours post transfection, Opti-MEM medium (Cat. #31985070, GIBCO) was discarded and refreshed with culture medium. 24 or 48 hours later, cells were processed for the following experiments.

Immunoprecipitation (IP) and western blot

HEK293T cells were transfected with indicated constructs for 48 hours. Peritoneal macrophages or transfected 293T cells were washed three times with ice-cold PBS and lysed with lysis buffer (Cat. #C500005, Sangon Biotech,) containing 1% (v/v) protease inhibitor cocktail (Cat. #P8340, Merck) for 30 min on ice, followed by centrifugation at 4°C to remove cell debris. A part of lysates was saved and used as input. The rest lysates was incubated with Anti-Flag (Cat. #A2220, Merck) or HA M2 affinity gel (Cat. #AT0079, CMCTAG) for 293T cells, or incubated with rabbit IgG (Cat. #17-5138-01GE Healthcare,) or TREM-2 antibodies (Cat. #ab269868, ABCAM) along with protein A plus G agarose beads (Calbiochem, USA) for BMDM cells, and then rotated overnight at 4 °C. The precipitated proteins were boiled in loading buffer after washes and analyzed by western blot. Equivalent amount (20 µg) of protein extracts were separated by SDS-PAGE electrophoresis and then transferred to polyvinylidene difluoride (PVDF) membrane. Membranes were blocked in PBS-Tween20 (pH 7.4, 0.5% Tween20) containing 5% BSA for 1 hour at room temperature (RT) and then incubated overnight at 4 °C with primary antibodies against TREM2 (Cat. #MABN755, Merck), BTK (Cat. #8547, CST), p-BTK (Cat. #87141S, CST), SHP1 (Cat. #3759, CST), p-SHP1 (Cat. #8849, CST), AMPK α (Cat. # 5831T, CST), p-AMPK α (Cat. #2535T, CST), STAT6 (Cat. #5397S, CST), p-STAT6 (Cat. #56554S, CST), HK2 (Cat. #2867S, CST), PKM2 (Cat. #4053S, CST), CPTI

(Cat. #ab128568, ABCAM), PPAR α (Cat. ab215270, ABCAM), PPAR β (Cat. #ab23673, ABCAM), PPAR γ (Cat. #ab45036, ABCAM), PGC1 α (Cat. ab54481, ABCAM), PGC1 β (Cat. #ab176328, ABCAM), HA-Tag (Cat. #3724S, CST), Flag-Tag (Cat. #2368S, CST), Myc-Tag (Cat. #2276, CST) and β -actin (Cat. #ab6276, ABCAM). Then the membranes were incubated with appropriate horseradish peroxidase (HRP)-conjugated secondary antibodies at RT for 1 hour, followed by the visualization with GE Image Quant LAS 500 using an ECL kit (Fdbio Science).

RNA sequencing

RNA sequencing was performed as previously described (2). Total RNA from healthy controls and sepsis patients was extracted using TRIzol reagent (Thermo Fisher) and were assessed for quantity and quality using a NanoDrop UV spectrophotometer and a Bioanalyser. The 4 RNA-seq libraries were sequenced on the Illumina NextSeq 500 platform at Sun-yat sen University, to produce over 60 million, 100 nucleotide paired-end reads per sample. Sequences were aligned to the reference human genome version GRCh38 using STAR. Gene expressions were obtained both as readcount directly from STAR as well as computed using RSEM in order to obtain gene and transcript level expression, either in TPM or FPKM values, for these stranded RNA libraries. Sample clustering based on normalized log readcounts produces the hierarchy of samples.

Protein structure prediction and visualization

The monomer structures of TREM2 and SHP1 were predicted using the Alphafold2 online tool (<https://www.bkunyun.com/>). The highest rated “rank0.pdb” file was selected for later analysis. The charge distribution and potential in protein structure was visualized and analyzed using the Vacuum Electronics feature in PyMOL (version 2.5.7). Potential intermolecular interactions and molecular recognition sites were revealed through color coded isosurfaces (red and blue represented negatively

charged and positively charged regions, respectively). The molecular docking between TREM2 (201-230aa) and SHP1 was simulated using Autodock vina (version 4.2.5.1). The conformational file with the highest score was selected and protein docking was performed using MOE (version 2019.01) to obtain scoring information (Supplementary table). All representative structures were visualized and exported by PyMOL software.

ScRNA-seq data analysis

The single-cell RNA-seq gene expression dataset GSE207651 of sepsis was obtained from GEO. The samples were analyzed in the R package “Seurat” (3, 4). The genes expressed by each cell were greater than 500 and less than 7500. The mitochondrial content and hemoglobin content were less than 10% and 5%. In addition, the number of UMIs in each cell was greater than 1000 and less than 50000, and log₁₀ Genes per UMI (the gene numbers per UMI) was greater than 0.8. Finally, the doublets were filtered by DoubletFinder (5). After filtering, UMI counts were variance-stabilized using scTransform with variable features, while regressing out number of UMIs and mitochondrial fraction. The harmony package was used to integrate the datasets (6). The umap algorithm was used to perform an overall dimensionality reduction analysis. Louvain clustering was performed, and cell annotation was determined by the R package “singleR” (7) and canonical genes. The myeloid cell cluster of the CLP group was selected for further analysis. Similarly, we performed dimensionality reduction for the myeloid cell dataset. According to the expression level of TREM2, we divided the myeloid cell clusters into TREM2 low and TREM2 high subpopulations. Differentially expressed genes (DEG) between two groups were identified with FindMarkers.

Quantitative real time PCR

Total RNA was extracted from monocytes and peritoneal macrophages using Trizol reagent (Cat. # 15596018, Thermo Fisher) according to the manufacturer's instructions. cDNAs were synthesized from 1 µg total RNA using a First Strand cDNA Synthesis Kit (Cat. #K1621, Thermo Fisher). Quantitative real-time PCR was performed with cDNA, SYBR green PCR master mix (Cat. #A6002, Promega) and primers for IL-1 β , IL-6 and IL-10 and detected with a CFX96 RT-PCR Detection System (Bio-Rad). Relative expression of target genes relative to β -actin was calculated.

Flow cytometry

The procedure of cell staining and flow cytometry was performed as previously described (8). Fluorescent dye-labelled Abs were purchased as following indicated: Anti-human antibodies: CD11b (Clone M1/70, Biolegend), CD14 (Clone HCD14, Biolegend), TREM2 (Clone 237920, R&D Systems), CD63 (Clone H5C6, Biolegend), CD9 (Clone HI9a, Biolegend), CD36 (Clone 5-271, Biolegend), CPTI (Clone 8F6AE9, ABCAM), CPTII (Clone 1C2AE6, ABCAM) and goat anti mouse IgG (Cat. #405308, Biolegend). Anti mouse antibodies: CD11b (Clone M1/70, BD Biosciences), Gr-1 (Clone RB6-8C5, eBioscience), F4/80 (Clone BM8, Biolegend), TREM2 (Clone 237920, R&D Systems), CD63 (Clone NVG-2, Biolegend), CD9 (Clone MZ3, Biolegend), MHC-II (Clone AF6-120.1, Biolegend), CD86 (Clone GL-1, Biolegend), ly6c (Clone HK1.4, Biolegend), TNF- α (clone MP6-XT22, Biolegend), IL-6 (Clone MP5-20F3, Biolegend) and IL-1 β (clone SB/199, Invitrogen). For intracellular TNF- α , IL-1 β and IL-6 staining, cells were restimulated with 50 ng/ml PMA (Cat. # P8139, Sigma), 1 µg/ml ionomycin (Cat. #I3909, Merck,) and 1 µg/ml brefeldin A (Cat. # 555029, BD) for 6 hours, and processed for the intracellular staining with fixation/permeabilization buffer set (eBioscience, CA, USA). A total of 500,000 events were acquired for each sample.

Samples were detected on FACS Fortessa flow cytometer (BD) and analyzed with FlowJo software (Tree Star, version 10.0.7).

Metabolism assessment

Triglyceride concentration assay

Triglyceride levels in serum and liver suspension were measured using the Triglyceride Quantification Assay kit (Colorimetric Fluorometric) (Cat. #ab65336, ABCAM) according to the manufacturer's instructions.

Free Fatty Acid Uptake Assay

Uptake of free FAs was measured by free FA uptake assay fluorometric kit (Cat. #ab176768, Abcam). WT and TREM2^{-/-} BMDMs (1×10^5 /well) were stimulated with PBS or LPS, and incubated for 20 minutes at RT in the addition of lipase, followed by the addition of the fluorescent triglyceride Probe. After 1 hour of incubation, fluorescence density was detected (excitation 535 nm, emission 587 nm) using multifunctional microplate reader (BIOTEK Synergy HTX).

Fatty acid oxidation assay

Macrophages (1×10^5 cells/well) sorted from WT and TREM2^{-/-} sepsis mice, PBS or LPS treated peritoneal macrophages (1×10^5 cells/well) and BMDMs (1×10^5 cells/well) were seeded on XF96 cell culture microplates (Cat. #102601-100, Agilent), followed by the measurement on the Agilent Seahorse XFe96 Analyzers, by using the XF Palmitate-BSA FAO Substrate (Cat. #102720-100, Agilent) and Mito Stress Test Kit (Cat. #103015-100, Agilent) refer to the manufacturer's protocol. As for BTK inhibitor assay, BMDMs or peritoneal macrophages were pre-treated with LFM-A13 (Cat. #S7734, Selleck) and Ibrutinib for 1 hour, followed by the stimulation with LPS. After 12 hours, culture medium was replaced with substrate limited DMEM medium (A14430-01, Life Technologies)

containing 0.5 mM glucose (Cat. #G8769, Merck), 1 mM GlutaMAX (Cat. #3505061, Life Technologies), 0.5 mM carnitine (Cat. #C0283, Merck) and 1% FBS for 24 hours. Then the cells were washed 3 times and incubated for 1 h in 1x KHB FAO assay buffer (111 mM NaCl, 4.7 mM KCl, 1.25 mM CaCl₂, 2 mM MgSO₄, 1.2 mM NaH₂PO₄) containing 2.5 mM glucose, 0.5 mM carnitine and 5 mM HEPES (15630080, Life Technologies) in a non CO₂ incubator at 37 °C. 30uL1 mM palmitate-BSA or BSA control was added immediately prior to beginning the assay. Three or more consecutive Oxygen consuming rate (OCR) measurements were conducted under basal conditions and after the sequential addition of 1 μM oligomycin, 0.5 μM FCCP and 0.5μM Rotenone/ antimycin A.

Glycolysis assay

Glycolysis of cells mentioned above was evaluated by the measurement of Extracellular Acidification Rate (EACR) using Agilent Seahorse XF Glycolysis Stress Test Kit (Cat. #103020-100, Agilent). Peritoneal macrophages (1x10⁵ cells/well) or BMDMs (1x10⁵ cells/well) were seeded on XF96 cell culture microplates either in the presence of PBS or LPS for indicated time. Before the detection with Agilent Seahorse XFe96 Analyzers, cells were washed 3 times and incubated for 1 hour in XF assay medium (Cat. #102035-100, Agilent) containing 1 mM L-glutamine (Cat. #G8540, Merck). Three or more consecutive ECAR measurements were obtained under basal conditions and after the sequential addition of 10mM Glucose, 2 μM oligomycin and 50 mM 2-DG.

Enzyme-linked immunosorbent assay (ELISA)

Serum, lung, liver and spleen were collected from sepsis mice at 24 hours post CLP. Lung, liver and spleen were homogenized in 2 ml PBS. Homogenized tissue supernatants were filtered by 0.22 μm membrane and collected. Concentrations of IL-1β, IL-6 and TNF-α were detected by mouse

IL-1 β (Dakewe, Cat#1210122), IL-6 (Dakewe, Cat#1210602) and TNF- α (Dakewe, Cat#1217202) ELISA kits bought from Dakewe biotech co., Ltd. according to the manufacturers' instructions.

LDH release assay

LDH release was measured by CytoTox96 Non-Radio Cytotoxicity Assay kit (Promega) in accordance with the manufacture's instruction. Cell culture supernatant was incubation with the substrate for 30min. After the stop of the reaction, and absorbance at 490nm was determined using a microplate reader. The percentage of LDH release (%) was calculated by the following formula, (Experimental LDH release / Maximum LDH release) \times 100 %, refer to the manufacturer's recommendations.

Colony forming units (CFU) assay

CFU assay was performed as previously described (1). In brief, spleen and lung sections were harvested from mice and weighed. Then tissues were lysed with 0.1%Triton-X100. Cell lysates in a series of 10-fold dilutions were plated in triplicate on *Pseudomonas* isolation agar, and then incubated overnight at 37°C. Survived bacteria per plate were counted and calculated.

ROS assay

ROS production was measured as previously described (1). Briefly, WT and TREM2^{-/-} BMDMs were either untreated (Ctrl) or treated with LPS for 12 hours, and cells were incubated with a ROS-sensitive probe 2', 7'-dichlorofluorescein diacetate (H2DCFDA, Cat. # D399, Thermofisher) at a concentration of 10 μ M. After that, cells were collected and washed 3 times, then analyzed using FACS Fortessa flow cytometer (BD). ROS levels were determined by the fluorescence of DCF, the deacetylated and oxidized product of H2DCFDA. Data were analyzed using FlowJo software (Tree Star, Version 10.0.7, USA).

Immunofluorescence assay

Cells were seeded on glass coverslips. After treatment, cells were fixed with 4% paraformaldehyde in PBS for 10 min at RT, followed by the permeabilization with 0.1% Triton X-100 in 5% BSA for 1 hour at RT. Then the fixed cells were incubated overnight with primary antibodies against BTK (Cat. # PA5-20085, ThermoFisher) and TREM2 (Cat. # AF1729, R&D Systems) or 2 μ g/mL BODIPY (D3922; Invitrogen, Thermo Fisher Scientific) at 4 °C, followed by the incubation with Alexa Fluor-488 and Alexa Fluor-594 conjugated anti-rabbit and mouse secondary antibodies (Invitrogen). After 4,6-diamidino-2-phenylindole (DAPI, Invitrogen) staining for 5 minutes, coverslips were mounted with ProLong Gold antifade reagent (Invitrogen). Fluorescence was visualized with a Zeiss LSM 880 confocal Microscope.

Histology analysis

For hematoxylin and eosin (H&E) staining, lung, liver and renal tissues of sepsis mice were immersed in 4% paraformaldehyde for 24h, next transferred to 70% ethanol, then dehydrated and embedded in paraffin. 5- μ m-thick lung tissue sections were dewaxed, rehydrated and washed, then stained with hematoxylin and eosin (H&E) to determine organ injuries and inflammatory cell infiltration. Images were captured with microscope (Olympus, U-RFL-T). Lung injuries are assessed according to the neutrophils number in the alveolar space and interstitial space, hyaline membranes, proteinaceous debris filling the airspaces and alveolar septal thickening as previously described (9). Histology score is determined and weighted according to the relevance ascribed to each feature and is normalized to the number of fields evaluated. The score is a continuous value between zero and one. Kidney injuries are scored according to the percentage of morphologic changes that displayed tubular cell necrosis, loss of brush border, vacuolization, tubule dilation, cast formation, and

inflammatory cells infiltration, as previously described (10). Score is determined as follows: 0, no damage; 1, mild damage; 2, degenerated cytoplasm with nucleus; 3, total necrosis without nucleus. The quantitative score was determined as follows: 0, no injury; 1, 1-25% damage; 2, 26-50% damage; 3, 51-75% damage; 4, damage over 75%. Liver injuries are evaluated according to the severity of necrosis, bleeding, and infiltration in the liver as previously described (11). Histology score was determined as follows: 0, no damage; 1, 1-25% damage; 2, 26-50% damage; 3, 51-75% damage; 4, 76-100% damage. The percentage of lesion area was calculated as the total lesion area divided by total surface area using Image J (12).

Oil Red O staining was performed in frozen liver sections to visualize the presence of neutral lipids. Liver tissues were fixed overnight with 10% neutral buffered formalin at 4°C. Fixed liver sections were washed twice and incubated in 30% sucrose for 24 hours, and then embedded in Optimal Cutting Temperature (OCT) compound to be frozen. Sectioned liver slices were stained with Oil red O, followed by the examination under a light microscope. Percentage of Oil Red O positive area were calculated in 10 fields in livers per group.

References

1. Ming S, Li M, Wu M, Zhang J, Zhong H, Chen J, et al. Immunoglobulin-Like Transcript 5 Inhibits Macrophage-Mediated Bacterial Killing and Antigen Presentation During Sepsis. *J Infect Dis.* 2019;220(10):1688-99.
2. Omer A, Barrera MC, Moran JL, Lian XJ, Di Marco S, Beausejour C, et al. G3BP1 controls the senescence-associated secretome and its impact on cancer progression. *Nat Commun.* 2020;11(1):4979.
3. Satija R, Farrell JA, Gennert D, Schier AF, and Regev A. Spatial reconstruction of single-cell gene expression data. *Nat Biotechnol.* 2015;33(5):495-502.
4. Butler A, Hoffman P, Smibert P, Papalexi E, and Satija R. Integrating single-cell transcriptomic data across different conditions, technologies, and species. *Nat Biotechnol.* 2018;36(5):411-20.
5. McGinnis CS, Murrow LM, and Gartner ZJ. DoubletFinder: Doublet Detection in Single-Cell RNA Sequencing Data Using Artificial Nearest Neighbors. *Cell Syst.* 2019;8(4):329-37 e4.
6. Korsunsky I, Millard N, Fan J, Slowikowski K, Zhang F, Wei K, et al. Fast, sensitive and accurate integration of single-cell data with Harmony. *Nat Methods.* 2019;16(12):1289-96.
7. Aran D, Looney AP, Liu L, Wu E, Fong V, Hsu A, et al. Reference-based analysis of lung single-cell sequencing reveals a transitional profibrotic macrophage. *Nat Immunol.* 2019;20(2):163-72.
8. Wu Y, Wu M, Ming S, Zhan X, Hu S, Li X, et al. TREM-2 promotes Th1 responses by interacting with the CD3zeta-ZAP70 complex following Mycobacterium tuberculosis infection. *J Clin Invest.* 2021;131(17).

9. Matute-Bello G, Downey G, Moore BB, Groshong SD, Matthay MA, Slutsky AS, et al. An official American Thoracic Society workshop report: features and measurements of experimental acute lung injury in animals. *Am J Respir Cell Mol Biol*. 2011;44(5):725-38.
10. Jia P, Teng J, Zou J, Fang Y, Wu X, Liang M, et al. Xenon Protects Against Septic Acute Kidney Injury via miR-21 Target Signaling Pathway. *Crit Care Med*. 2015;43(7):e250-9.
11. Ito S, Tanaka Y, Oshino R, Okado S, Hori M, and Isobe KI. GADD34 suppresses lipopolysaccharide-induced sepsis and tissue injury through the regulation of macrophage activation. *Cell Death Dis*. 2016;7:e2219.
12. Li Z, Zhao P, Zhang Y, Wang J, Wang C, Liu Y, et al. Exosome-based Ldlr gene therapy for familial hypercholesterolemia in a mouse model. *Theranostics*. 2021;11(6):2953-65.

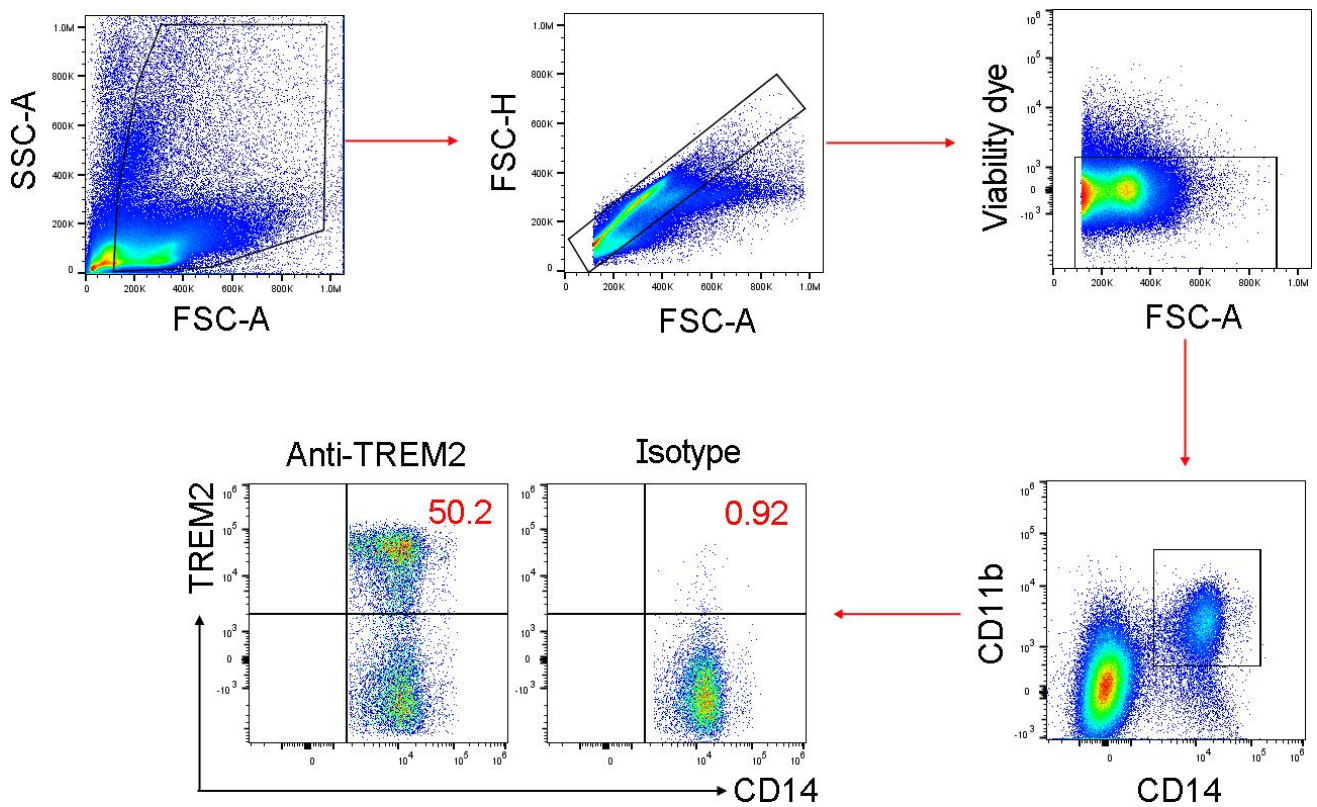


Figure S1, related to Figure 1. Gating strategies. PBMCs were gated as single, live (Viability dye⁻) cells. Monocytes were gated as CD11b⁺CD14⁺ cells. IgG isotype was used to set the cutoff value of TREM2⁺ cells and TREM2⁻ cells.

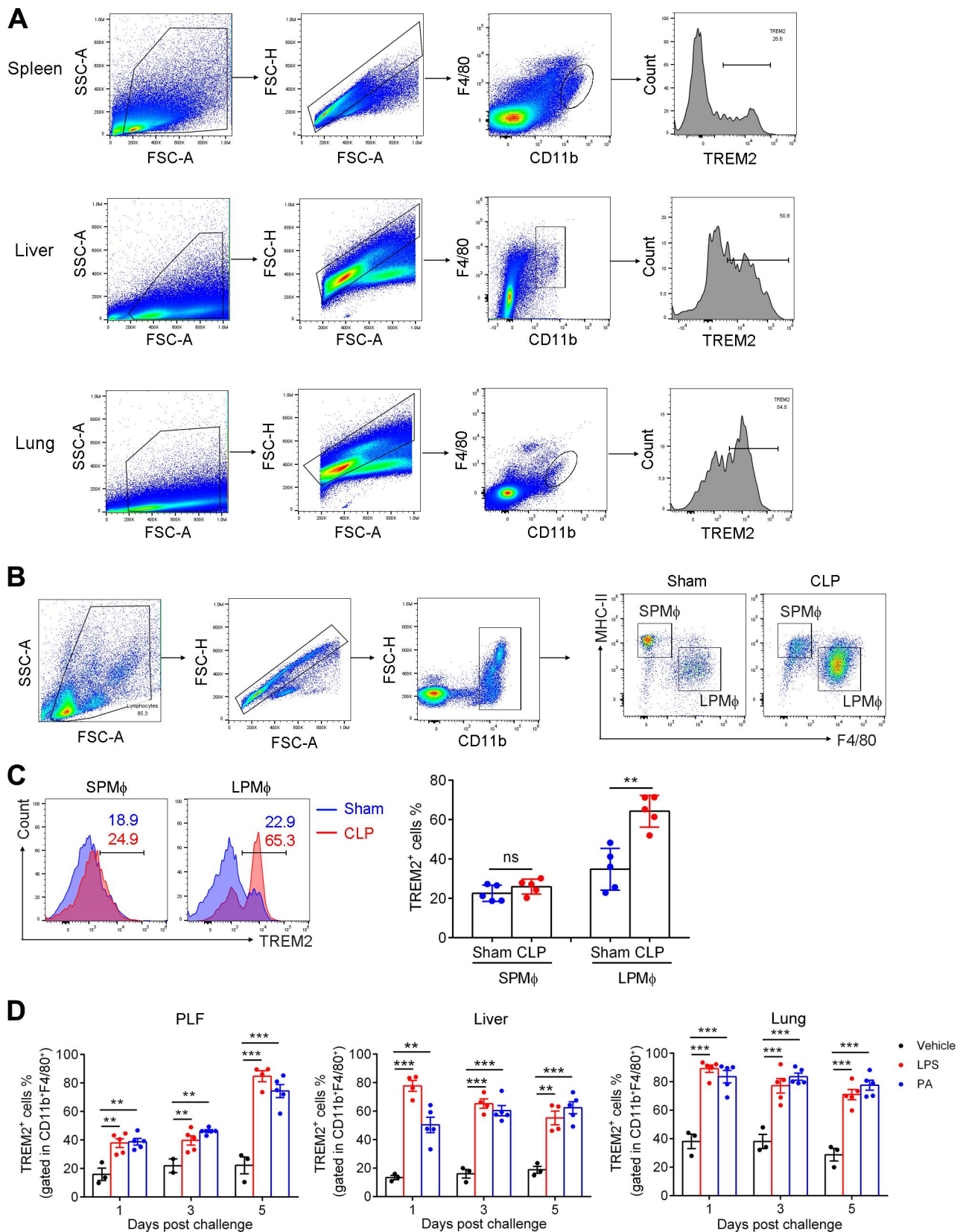


Figure S2, related to Figure 1. TREM2 expression was up-regulated on macrophages in CLP sepsis mouse model. A-D, CLP sepsis model was established in C57BL/6 mice. 24 hours later, (A)

TREM2 expressions on macrophages (Gated as CD11b⁺ F4/80⁺ cells) from lung, liver and spleen were determined by flow cytometry. **(B)** The percentages of large peritoneal macrophages (LPM ϕ) and small peritoneal macrophages (SPM ϕ) were shown. Peritoneal macrophages were gated as single and live CD11b⁺ cells. LPM ϕ and SPM ϕ were gated as F4/80^{high} MHC-II^{low} and F4/80^{low} MHC-II^{high} cells respectively. **(C)** TREM2 expressions in LPM ϕ and SPM ϕ from Sham or CLP sepsis model were determined by flow cytometry. **(D)** Endotoxemia mouse model and bacterial sepsis model were respectively established by the intraperitoneal (i.p.) injection of LPS (20mg/kg) or *P. aeruginosa* (PA) at a MOI of 1x10⁷ CFU/kg. TREM2 expressions in CD11b⁺ F4/80⁺ macrophages at day1, day 3 and day 5 post challenge were assessed in peritoneal lavage fluids (PLF), liver and lung by flow cytometry. Data represent the mean \pm s.e.m from three independent experiments. **, $P < 0.01$; ***, $P < 0.001$; ns, no significance.

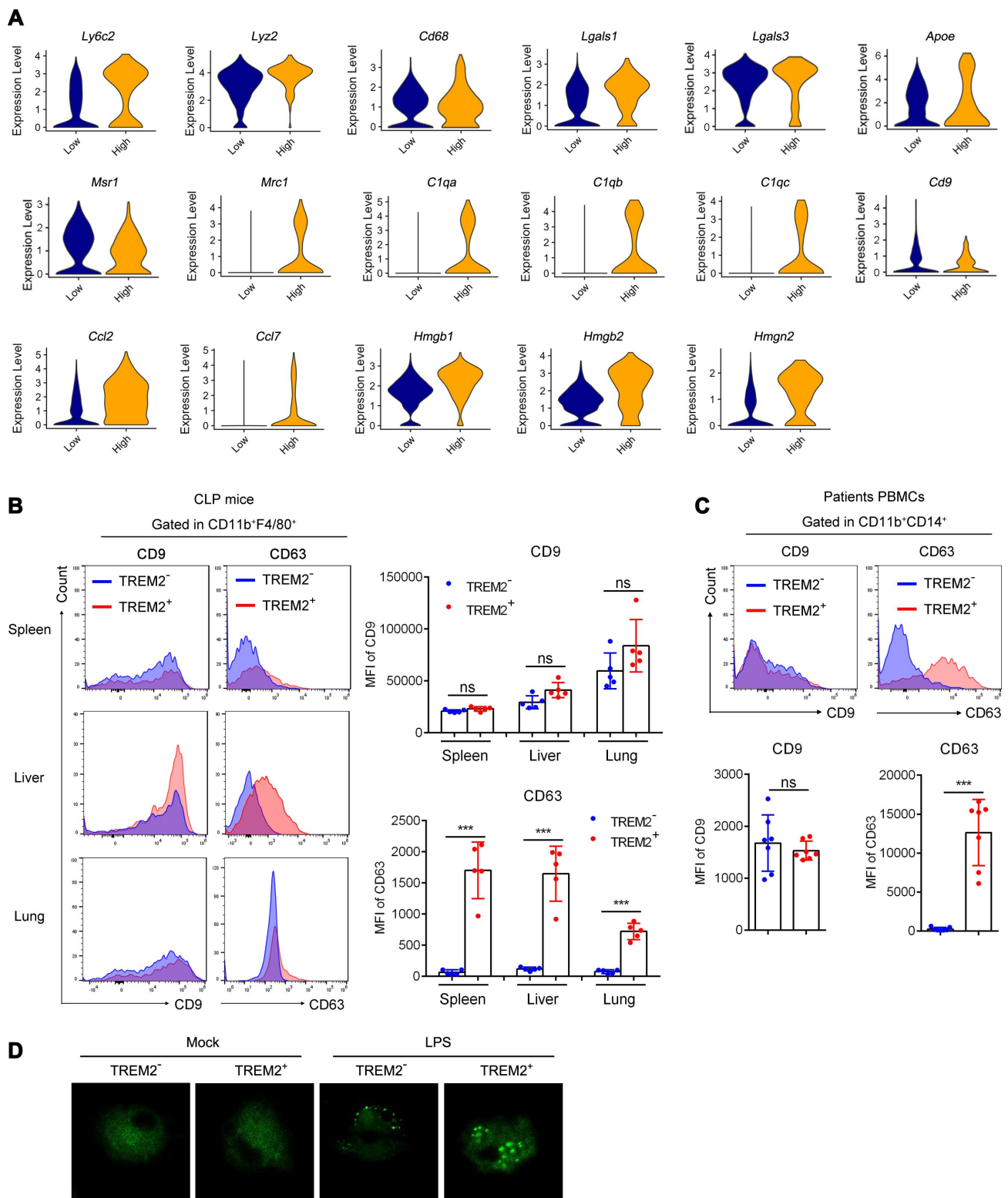


Figure S3, related to Figure 1. TREM2⁺ macrophages displayed lipid-associated phenotype during sepsis. (A) Single cell sequencing data from the lung of CLP sepsis mice were analyzed, and

violin plots for the expression of Ly6c2, Lyz2, Cd68, Lgals1, Lgals3, Apoe, Msr1, Mrc1, C1qa, C1qb, Cd9, Ccl2, Ccl7, Hmgb1, Hmgb2 and Hmgn2 in TREM2⁻ and TREM2⁺ macrophage clusters were shown. **(B)** CLP sepsis model was established. 24 hours later, expressions of CD9 and CD63 in TREM2⁻ or TREM2⁺ macrophages from lung, liver and spleen were detected by flow cytometry and the mean fluorescence intensities (MFI) of CD9 and CD63 were shown. **(C)** The expressions of CD9 and CD63 in TREM2⁻ or TREM2⁺ monocytes from sepsis patients (n=8) were analyzed by flow cytometry. **(D)** TREM2⁻ and TREM2⁺ macrophages were sorted from splenic cells and treated with vehicle (mock) or LPS (1µg/ml) for 12 hours, followed by the incubation with BODIPY lipid dye to determine the lipid uptake ability of macrophages. One way ANOVA was used in **B**. Unpaired student t test was employed in **C**. Data represent the mean ± s.e.m from three independent experiments. ***, $P < 0.001$; ns, no significance.

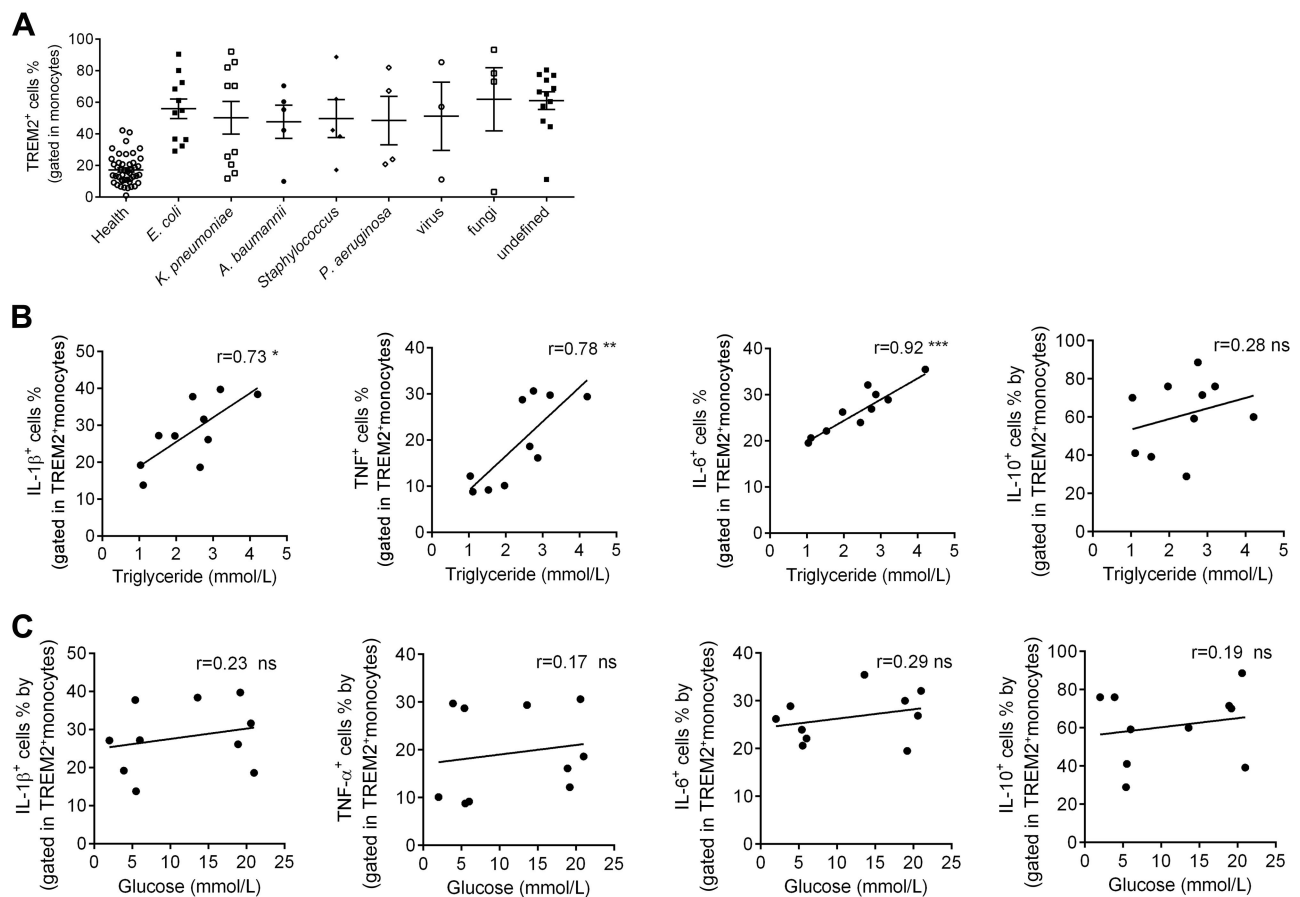


Figure S4, related to Figure 1. TREM2 expression was associated with disease severity in sepsis.

(A) Sepsis patients were classified into eight groups according to the types of infection and TREM2 expression in monocytes (Gated as CD11b⁺ CD14⁺ cells) was determined by flow cytometry. B-C, PBMCs were isolated from sepsis patients (n=10) and stimulated with LPS for 6 hours, followed by the detection of TREM2 expression and cytokines production. The correlations of serum triglyceride level (B) and glucose (C) level of sepsis patients with IL-1 β , IL-6, TNF- α and IL-10 produced by TREM2⁺ monocytes were analyzed. Spearman correlation analysis was used in B-C. Data represent the mean \pm s.e.m from three independent experiments. *, $P < 0.05$; **, $P < 0.01$; ***, $P < 0.001$; ns, no significance.

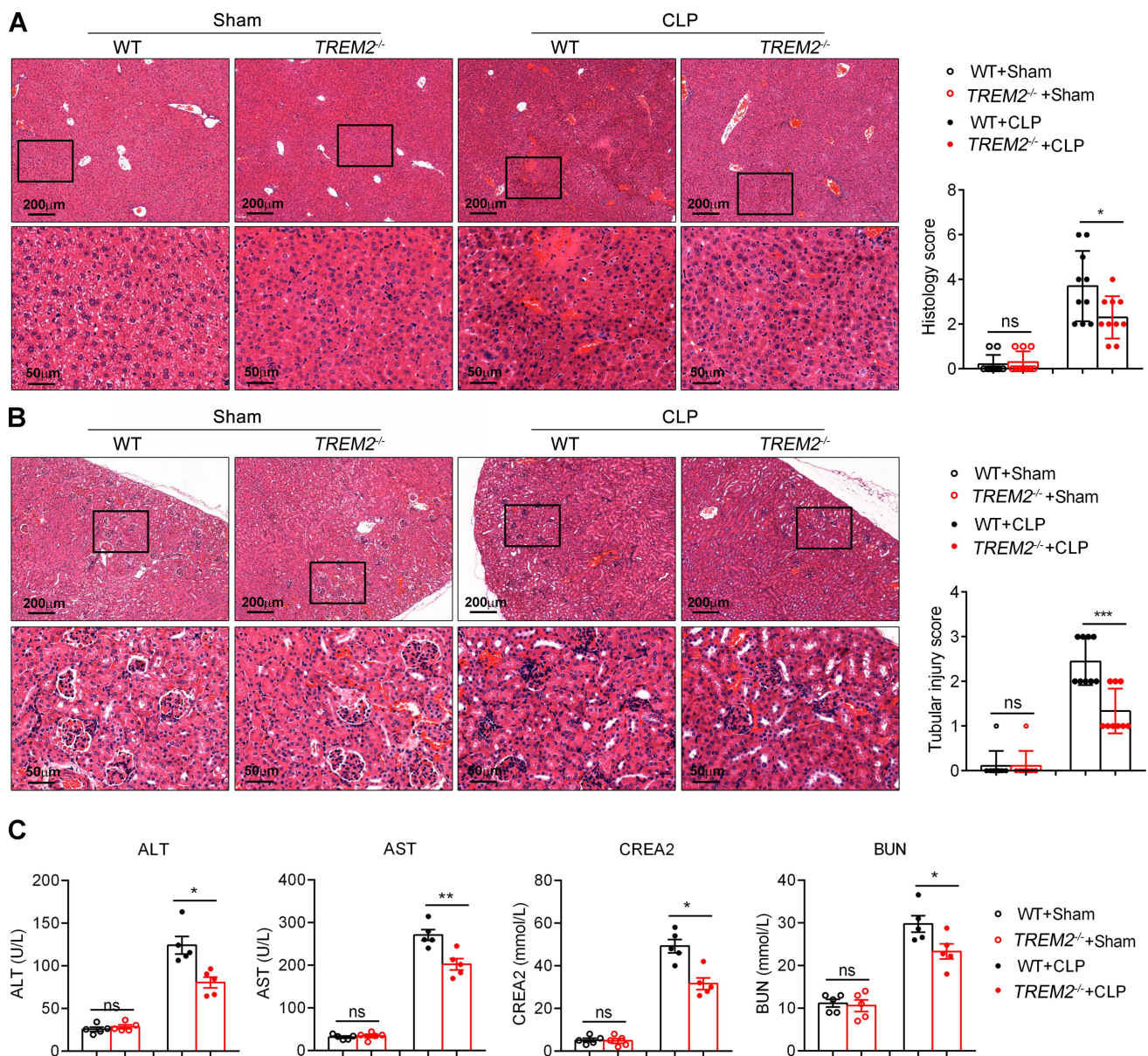


Figure S5, related to Figure 2. TREM2 knockout alleviates sepsis-induced organ damage. A-C, CLP sepsis model was established in WT and *TREM2*^{-/-} mice. Liver injuries (A) and renal damage (B) were evaluated by H&E staining after 24 hours. Scale bars, 50 μ m. (C) 24 hours later, serum levels of biochemical indexes including ALT, AST, CREA2 and BUN were detected. One way ANOVA was employed in A-C. Data represent the mean \pm s.e.m from three independent experiments. *, $P < 0.05$; **, $P < 0.01$; ***, $P < 0.001$; ns, no significance.

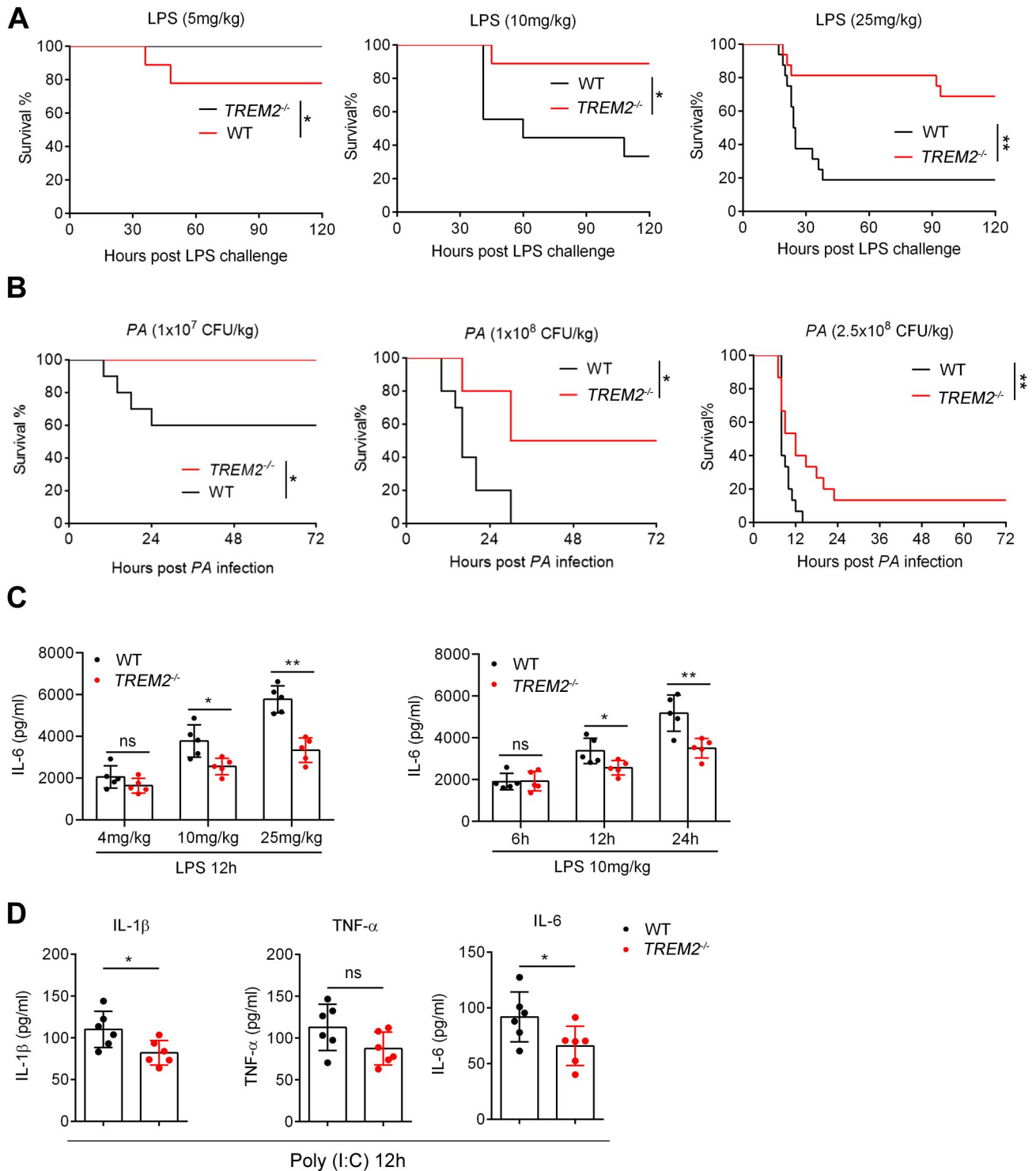


Figure S6, related to Figure 2. TREM2 knockout reduces mortality rate and alleviates systemic inflammation after LPS challenge and *PA* infection. A-B, Endotoxemia and bacterial sepsis models were established by i.p. injection of LPS (5mg/kg, 10mg/kg and 25 mg/kg) (A) or *PA* (1×10^7

CFU/kg, 1×10^8 CFU/kg and 2.5×10^8 CFU/kg) **(B)** in WT and TREM2^{-/-} mice. The survival rates were observed. **(C)** Endotoxemia mouse model was established in WT and TREM2^{-/-} mice (n=5 per group) with different doses of LPS. Serum IL-6 levels at indicated time points were determined by ELISA. **(D)** Poly (I:C) (30 mg/kg) were i.p. injected in WT and TREM2^{-/-} mice. Serum IL-6, TNF- α and IL-1 β levels were determined by ELISA 6 hours later. Long rank (Mantel Cox) test was adopted to compare the significance in **A** and **B**. One way ANOVA was used in **C**. Unpaired student t test was employed in **D**. Data represent the mean \pm s.e.m from three independent experiments. *, $P < 0.05$; **, $P < 0.01$; ns, no significance.

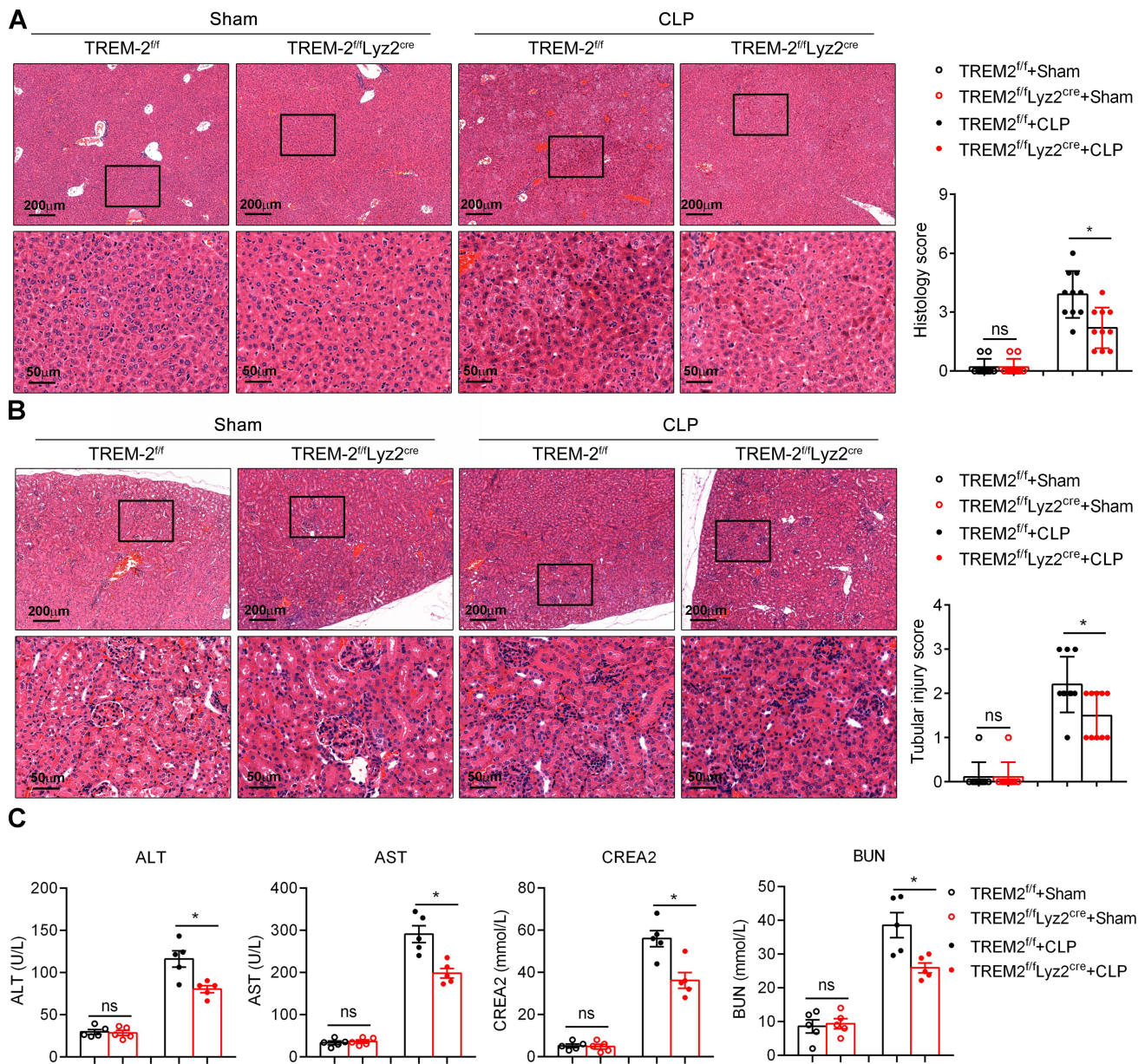


Figure S7, related to Figure 2. Conditional knockout of TREM2 in macrophages ameliorates sepsis-induced organ damage. A-C, CLP sepsis model was established in TREM2^{fl/fl} and TREM2^{fl/fl}Lyz2^{cre} mice. H&E staining was performed to assess the liver injuries (A) and kidney damage (B) 24 hours later. Scale bars, 50 μ m. (C) After 24 hours, serum was collected and the levels of biochemical indexes ALT, AST, CREA2 and BUN were detected. One way ANOVA was employed in A-C. Data represent the mean \pm s.e.m from three independent experiments. *, $P < 0.05$; ns, no significance.

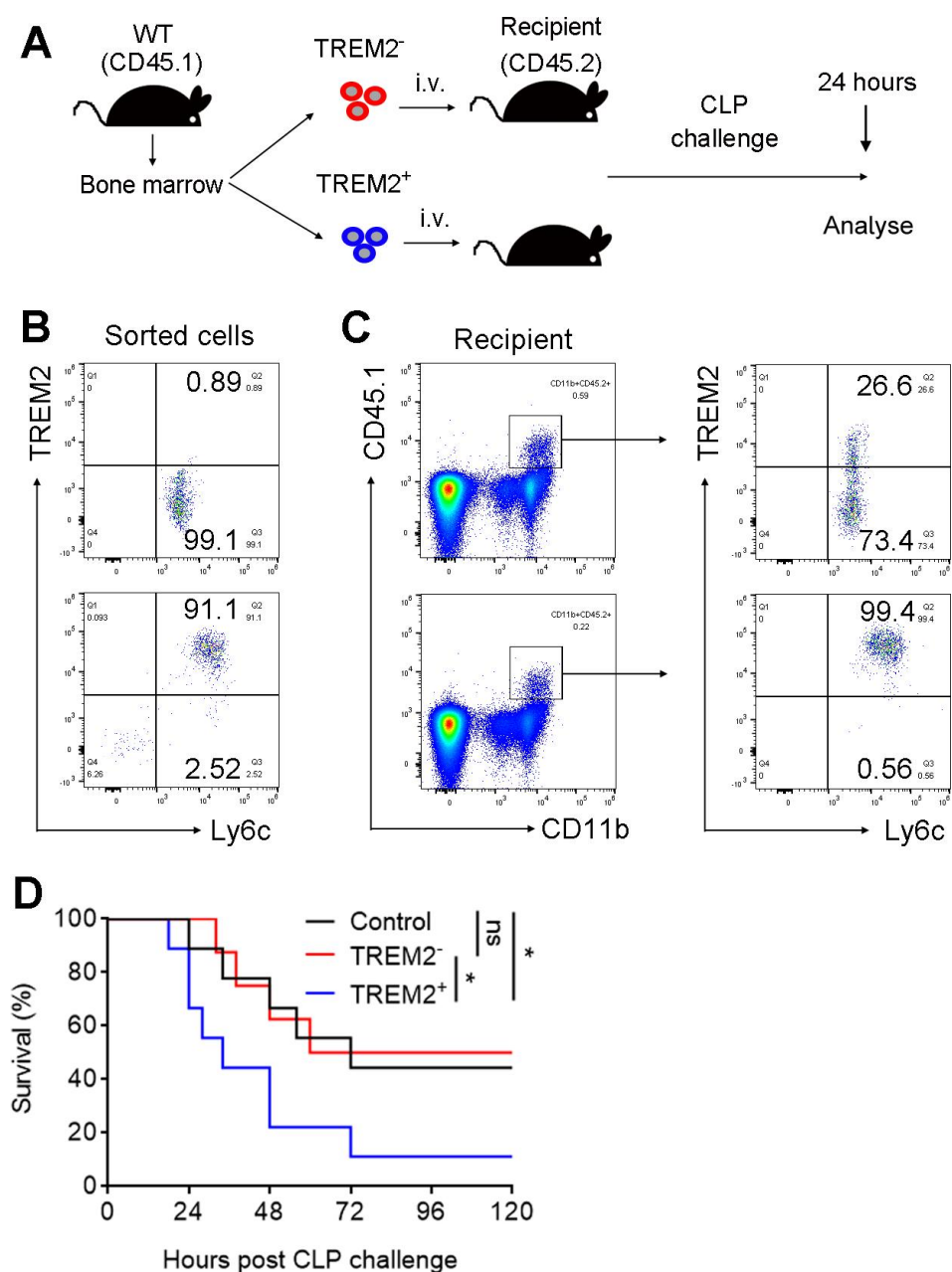


Figure S8, related to Figure 2. TREM-2 expression induction and stability in monocyte after CLP challenge. A-D, TREM2⁻ or TREM2⁺ monocytes were sorted from bone marrow of CD45.1 transgenic mice and transferred into CD45.2 recipient mice (5×10^6 cells/mice). 24 hours post transfer, recipient mice were challenged with CLP. (A) Schematic graph for the adoptive transfer assay. (B) The phenotype of sorted monocytes was confirmed by flow cytometry. (C) TREM2 expression on transferred CD45.1⁺CD11b⁺Ly6c⁺ monocytes in recipient mice was determined at 24 hours after CLP.

(D) CLP sepsis model was established in recipient mice transferred with TREM2⁻ or TREM2⁺ monocytes. The survival rates were observed. Long rank (Mantel Cox) test was adopted to compare the significance in **D**. Data represent the mean \pm s.e.m from three independent experiments. *, $P < 0.05$; ns, no significance.

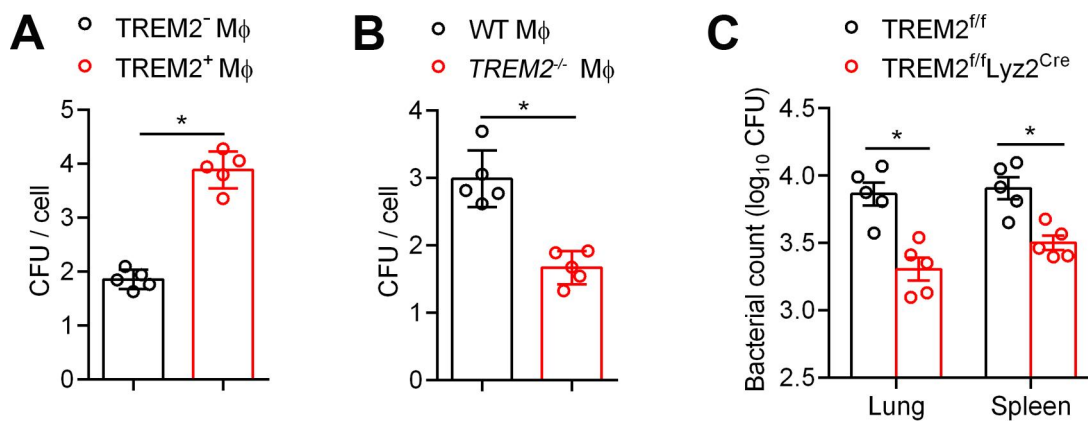


Figure S9, related to Figure 2. Deficiency of TREM2 increased the bacterial clearance of *PA* in vitro and in vivo. A-B, CLP sepsis model was established. TREM2⁻ vs TREM2⁺ (A) or WT vs TREM2^{-/-} (B) macrophages (gated in CD11b⁺F4/80⁺) were sorted from spleen and infected with *PA* at a MOI of 10 CFU/cell. 24 hours later, bacterial counts were determined by CFU assay. (C) TREM2^{fl/fl} vs TREM2^{fl/fl}Lyz2^{cre} mice were infected with *PA* (i.p.) at a MOI of 1x10⁷ CFU/kg. Bacterial counts were determined in the lung and spleen of mice 24 hours later. Unpaired student t test was employed in A-B. One way ANOVA was performed in C. Data represent the mean ± s.e.m from at least three independent experiments. *, P < 0.05.

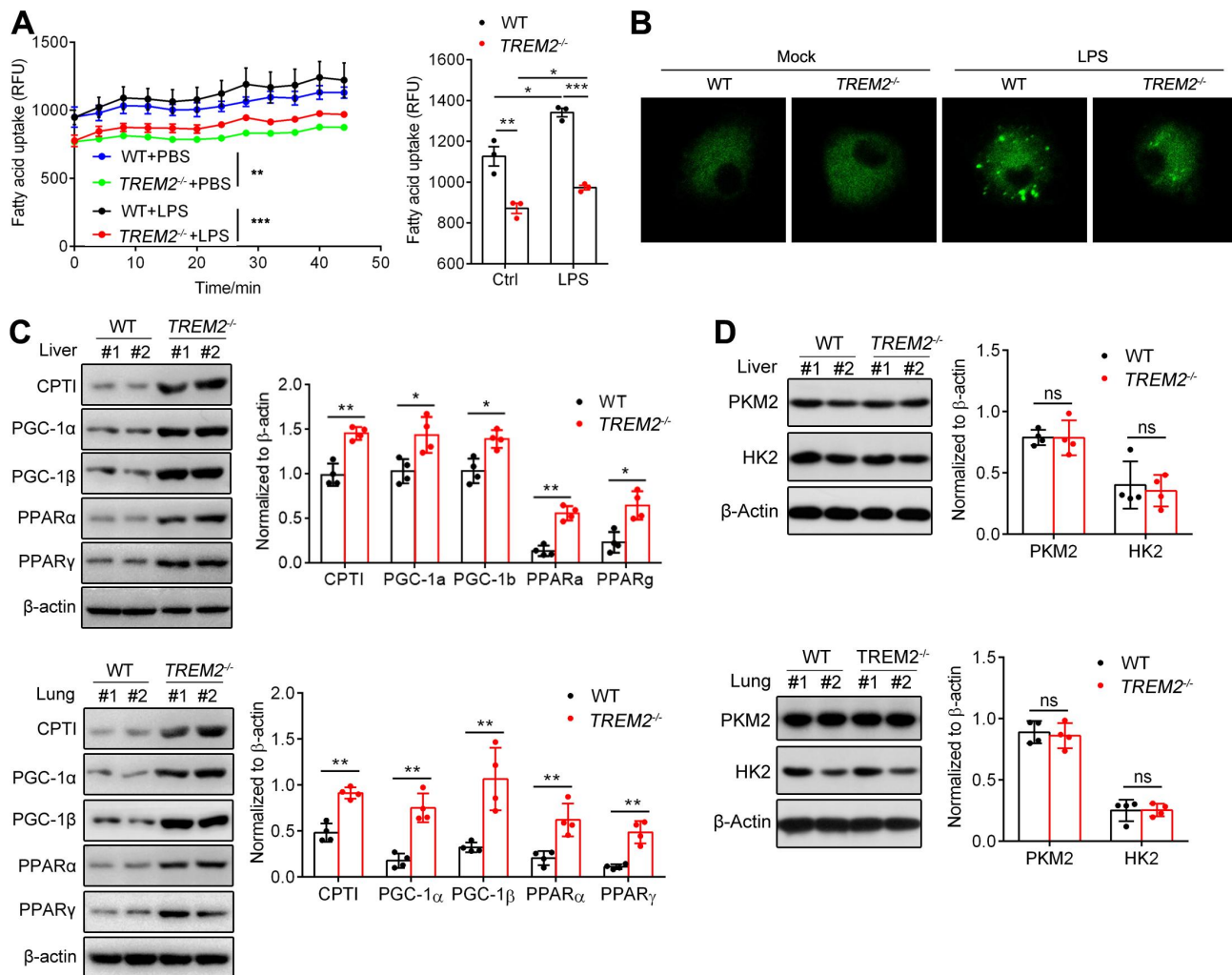


Figure S10, related to Figure 3. TREM2 deficiency promotes fatty acid oxidation in sepsis.

A-B, WT and TREM2^{-/-} BMDMs were stimulated with vehicle (mock) or LPS (1 μg/ml) for 12 hours. **(A)** Fatty acid uptake was measured by fluorometric method. **(B)** Immunofluorescence was performed with BODIPY dye to determine the uptake of lipid. **C-D**, CLP mouse model was established in WT and TREM2^{-/-} mice. 24 hours later, **(C)** Expressions of FAO rate-limiting enzyme CPTI and FAO-associated molecules including PGC-1 and PPAR in the lung and liver were assessed by western blot. **(D)** Expressions of rate-limiting enzymes of glycolysis (HK2, PKM2) in the lung and liver were detected. Gray scanning of western blot bands was performed and calculated by Image J software. One way ANOVA was used to analyze the significance in **A**. Unpaired student t

test was performed in **C** and **D**. Data represent the mean \pm s.e.m from three independent experiments.

*, $P < 0.05$; **, $P < 0.01$; ***, $P < 0.001$; ns, no significance.

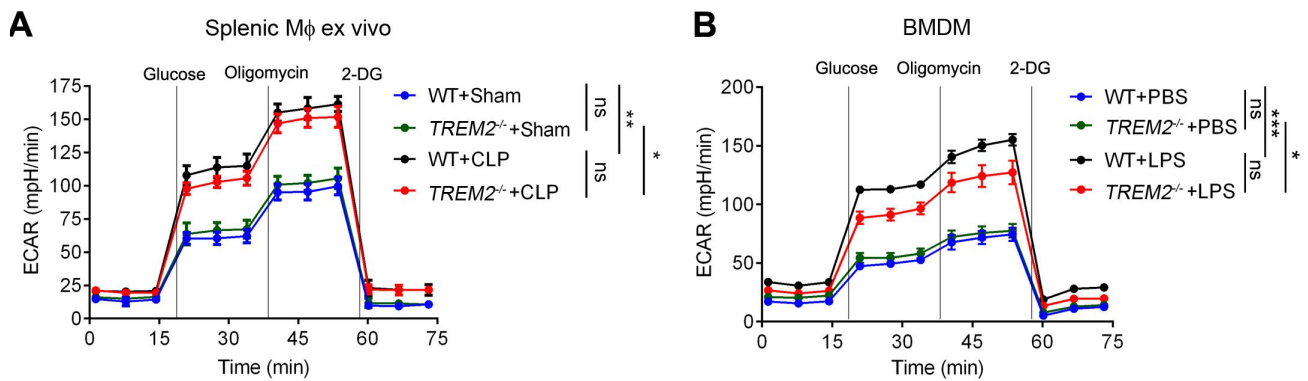


Figure S11, related to Figure 3. TREM2 deficiency did not affect the glycolysis of macrophages.

(A) CLP mouse model was established in WT and *TREM2*^{-/-} mice. Splenic macrophages were isolated and the rate of glycolysis was determined by Seahorse XF Extracellular Flux Analyzers. (B) BMDMs were isolated and stimulated with LPS (1 μ g/ml) for 12 hours, and then tested for the cellular glycolysis level. Two way ANOVA was used to analyze the significance in A and B. Data represent the mean \pm s.e.m from three independent experiments. *, $P < 0.05$; ***, $P < 0.001$; ns, no significance.

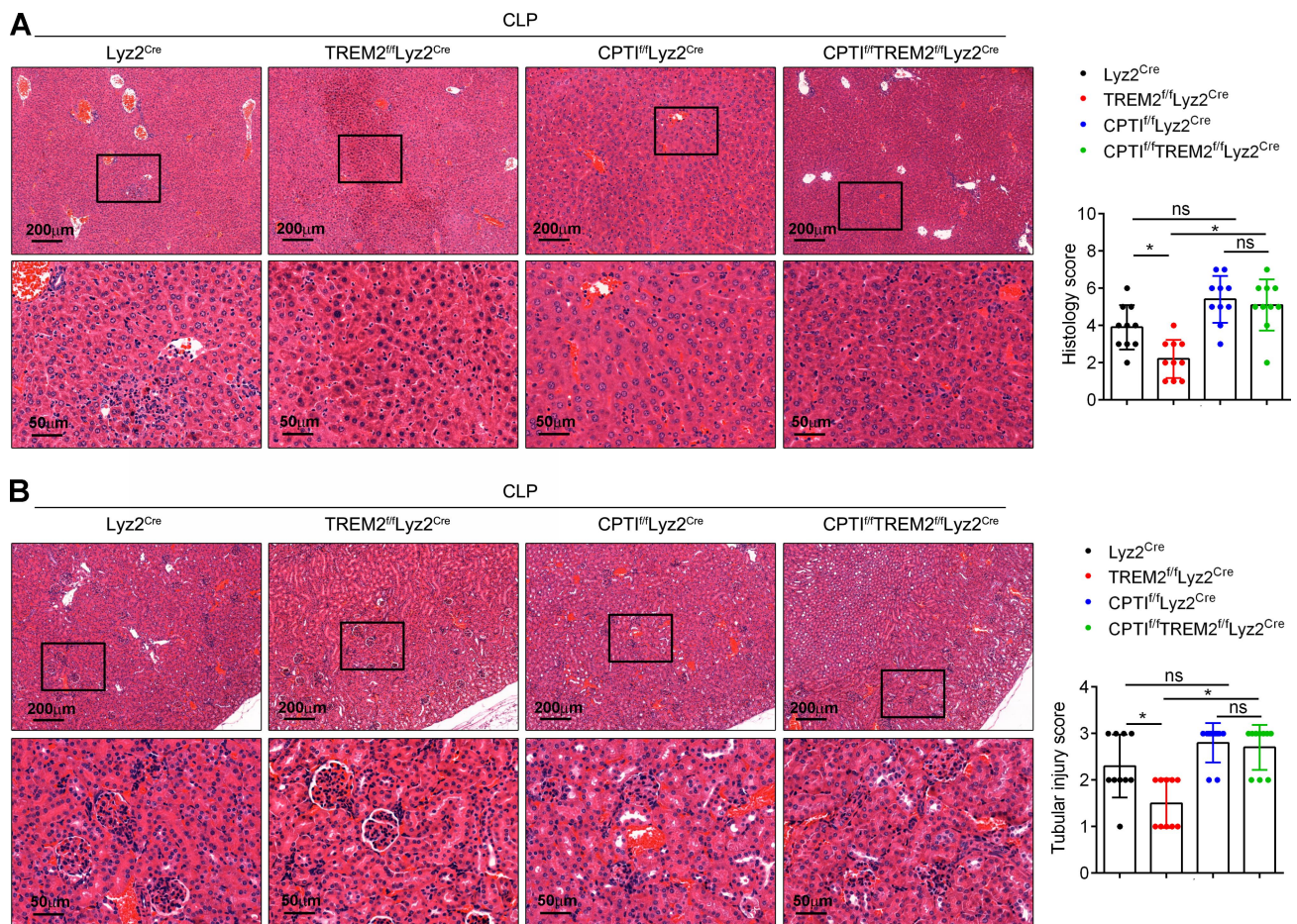


Figure S12, related to Figure 4. Double knockout of CPT1 and TREM2 in macrophages accelerates sepsis-induced organ damage. CLP sepsis model was established in Lyz2^{Cre}, TREM2^{ff}/Lyz2^{Cre}, CPT1^{ff}/Lyz2^{Cre} and CPT1^{ff}TREM2^{ff}/Lyz2^{Cre} mice. Liver injuries (**A**) and renal damage (**B**) were evaluated by H&E staining 24 hours post CLP. Scale bars, 50 μ m. One way ANOVA was employed in **A** and **B**. Data represent the mean \pm s.e.m from three independent experiments. *, $P < 0.05$; ns, no significance.

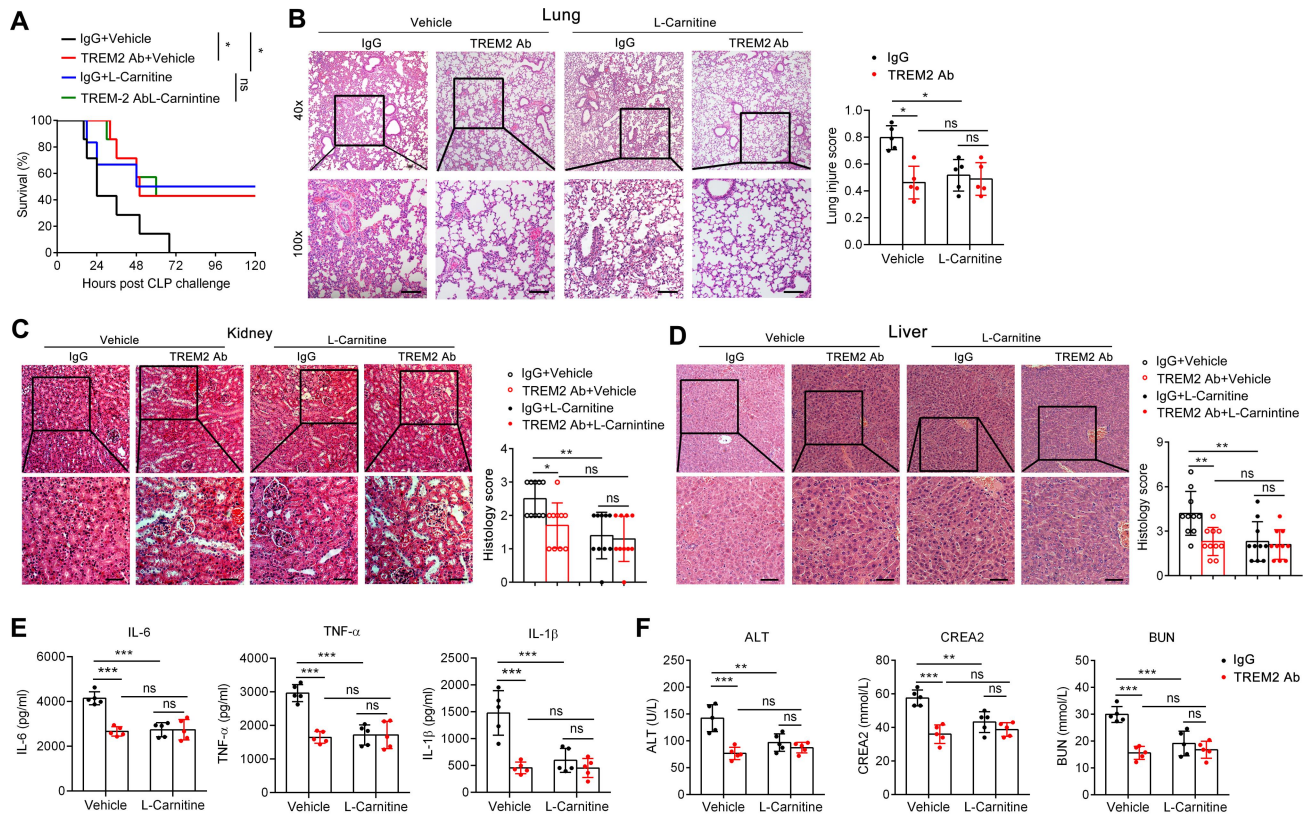


Figure S13, related to Figure 4. TREM2 blockade has a comparably beneficial effect with L-carnitine supplementation in sepsis alleviation. CLP sepsis mouse model was established in mice receiving L-carnitine (500mg/kg) or TREM2 blocking Ab (150mg/kg). **(A)** The survival rates were observed. **(B-D)** H&E staining was performed to evaluate the lung **(B)**, kidney **(C)** and liver **(D)** injuries 24 hours later. **(E)** Serum IL-6 and IL-1 β levels were determined by ELISA 24 hours later. **(F)** Serum ALT, CRP, CREA2 and BUN concentrations were determined 24 hours later. Long rank (Mantel Cox) test was adopted to compare the significance in **A**. One way ANOVA was employed in **B-F**. Data represent the mean \pm s.e.m from at least three independent experiments. Scale bars, 100 μ m for B and 50 μ m for C and D. *, $P < 0.05$; **, $P < 0.01$; ***, $P < 0.001$; ns, no significance.

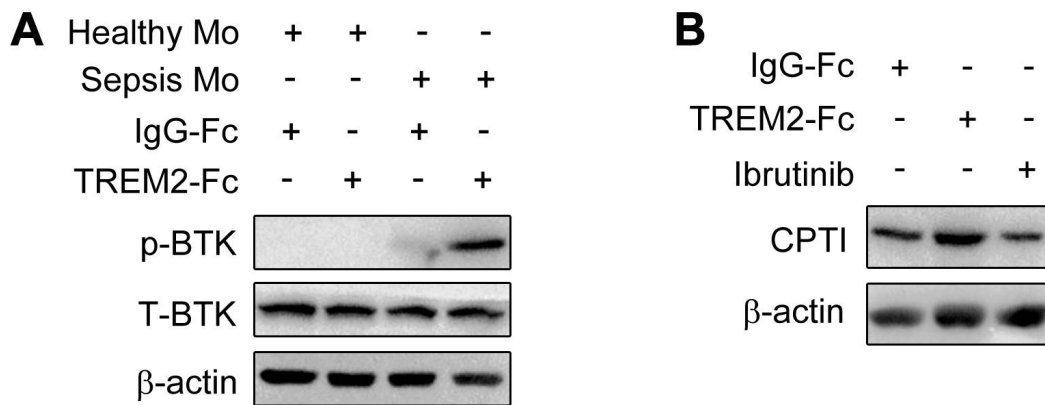


Figure S14, related to Figure 5. TREM2 inhibits BTK phosphorylation and CPTI expression in monocytes from sepsis patients. (A) CD14⁺ monocytes were sorted from PBMCs of sepsis patients or healthy donors and treated with recombinant TREM2-Fc protein (4μg/mL) or IgG-Fc for 12 hours, followed by the detection of the phosphorylated and total levels of BTK by western blot. **(B)** CD14⁺ monocytes were isolated from sepsis patients. After the pretreatment with Ibrutinib (1μM) for 1 hour, monocytes were stimulated with LPS in the presence of recombinant TREM2-Fc protein (4μg/mL) or IgG-Fc for 12 hours. The expression of CPTI was detected by western blot.

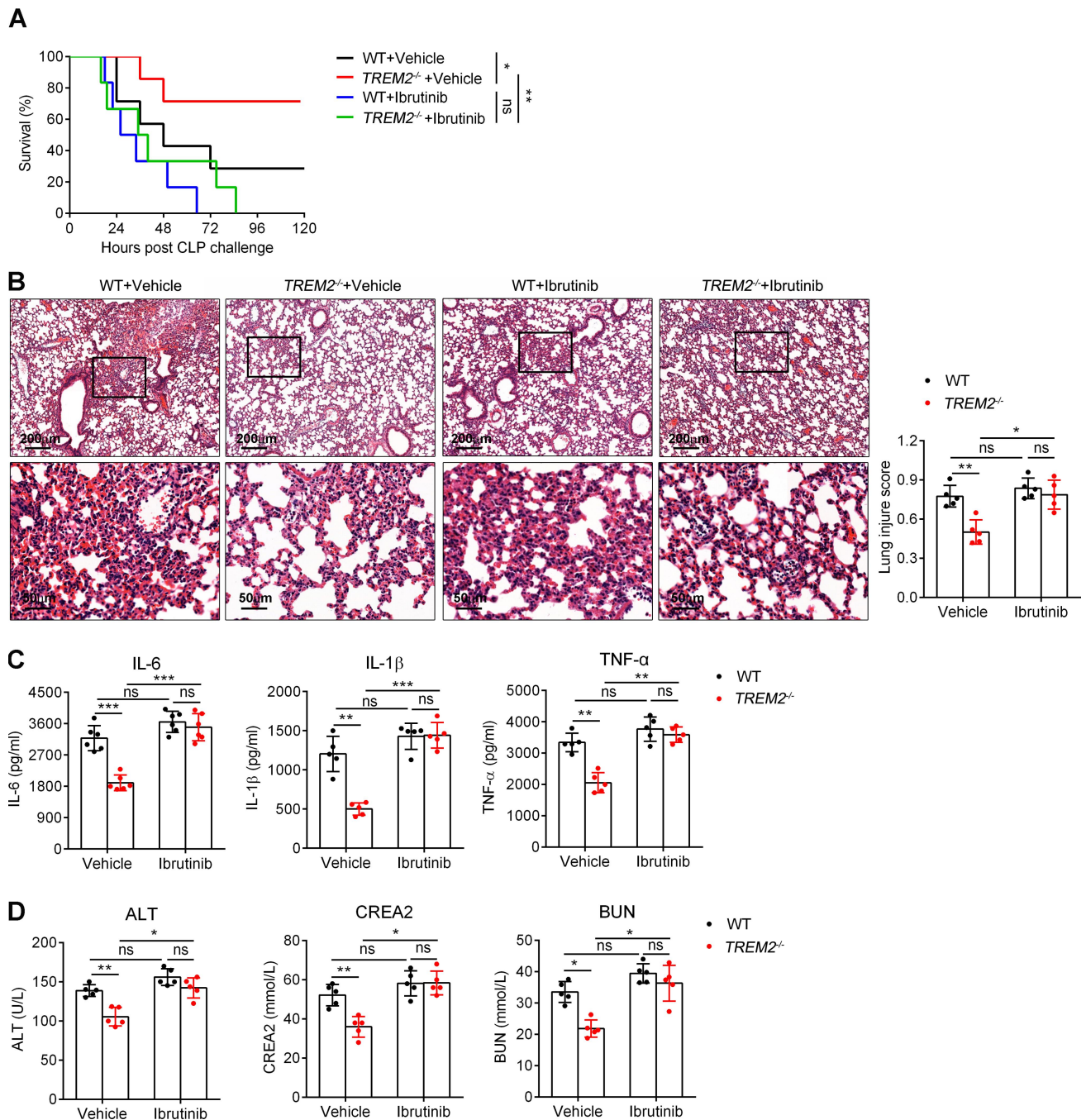


Figure S15, related to Figure 5. BTK inhibitor abolishes the protective effects induced by TREM2 deficiency. A-D, WT and *TREM2*^{f/f}*Lyz2*^{cre} mice were treated with Ibrutinib (5mg/kg) for 2 hours, followed by the challenge of CLP. (A) The survival rates were observed. (B) After 24 hours, H&E staining was performed to assess the lung injuries and inflammatory cell infiltration. Scale bars, 50µm. (C) Serum IL-6 and IL-1β levels were determined by ELISA 24 hours later. (D) ALT, BUN and CREA2 concentrations in serum were detected 24 hours later. Long rank (Mantel Cox) test was

adopted to compare the significance in **A**. One way ANOVA was employed in **C** and **D**. Data represent the mean \pm s.e.m from at least three independent experiments. *, $P < 0.05$; **, $P < 0.01$; ***, $P < 0.001$; ns, no significance.

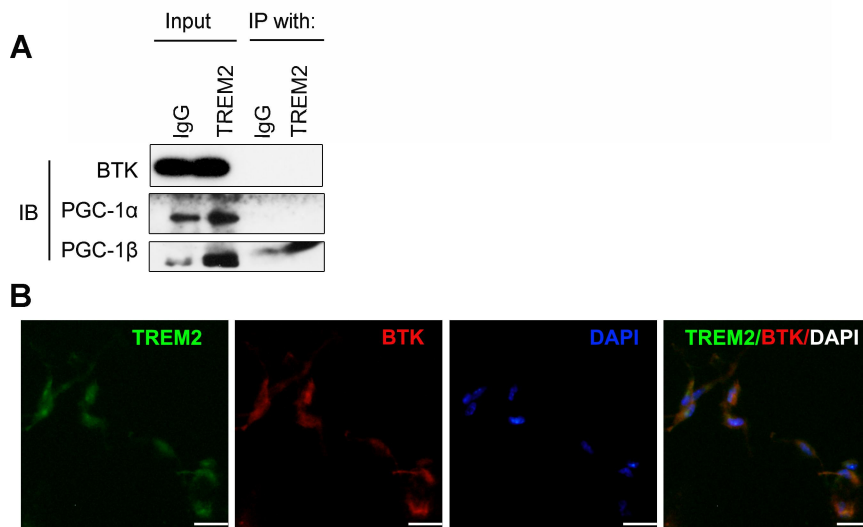


Figure S16, related to Figure 6. TREM2 did not interact with BTK. (A) BMDM cells were lysed and immunoprecipitated with IgG or TREM2 antibody. The interactions of TREM2 with BTK, PGC-1 α and PGC-1 β were determined by western blot. **(B)** Immunofluorescence was performed in BMDMs to determine the co-localization of TREM2 (Green) with BTK (Red). Nucleus was stained with DAPI (Blue). Scale bars, 20 μ m.

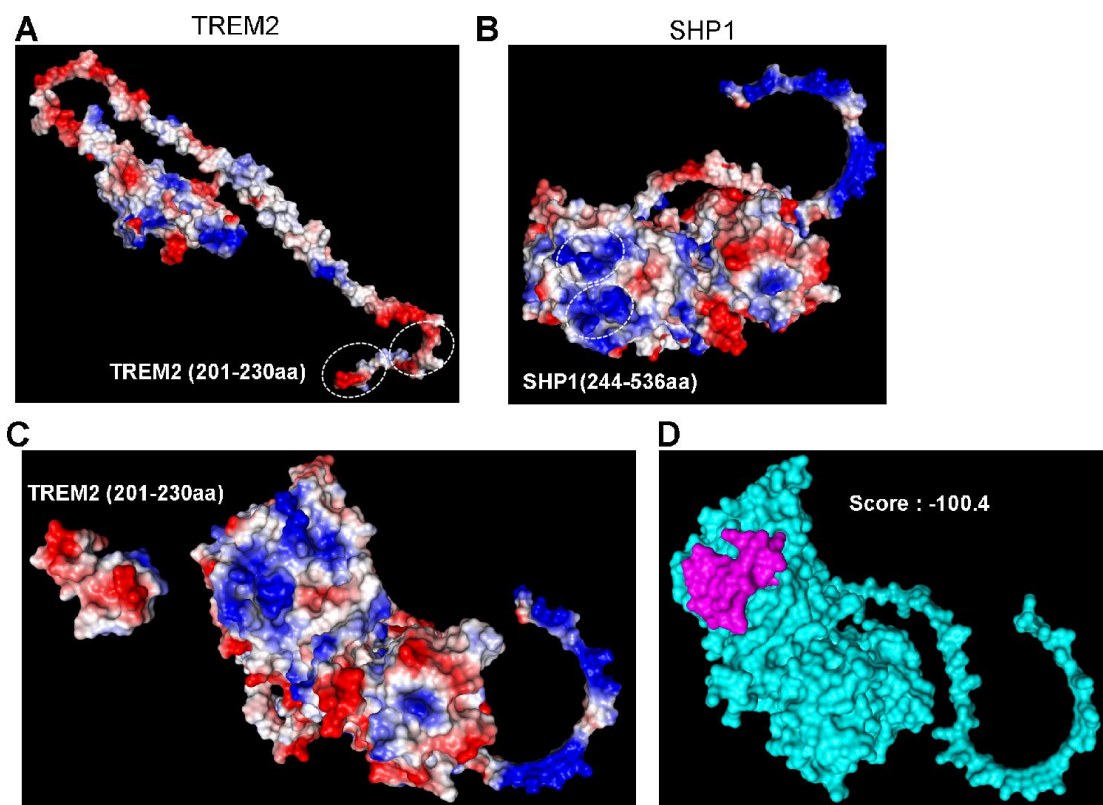


Figure S17, related to Figure 6. Structure prediction of the interaction between TREM2 and SHP1. (A) Charge distribution and potential in TREM2 structure. **(B)** Charge distribution and potential in SHP1 structure. The white oval dashed box of A and B marked the potential molecular surfaces involved in molecular docking. **(C)** Charge distribution and potential in TREM2 (201-230aa) and SHP1 structures after docking. TREM2 (201-230aa) shown was the structure after a horizontal flip of 180 degrees. **(D)** TREM2 (201-230aa) and SHP1 structures after docking. TREM2 (201-230aa) and SHP1 structures were rendered in magentas and ayans, respectively. Displayed score was the highest ranked scoring result.

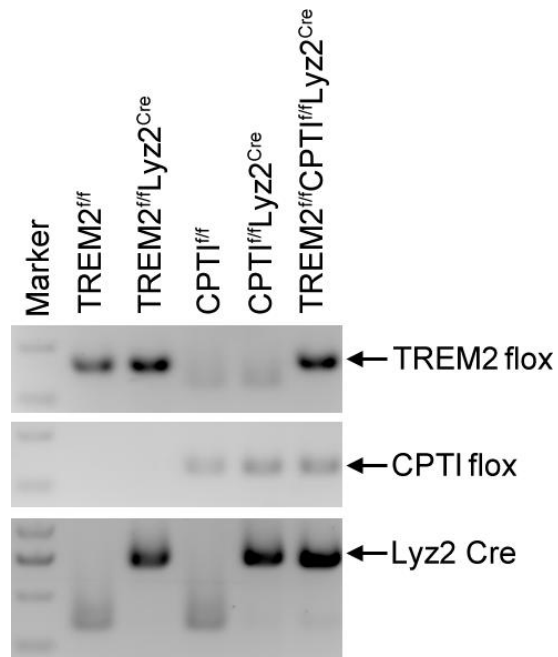


Figure S18. Identification of gene knockout mice. The gene phenotypes of TREM2^{fl/fl} mice, TREM2^{fl/fl}Lyz2^{cre} mice, CPT1^{fl/fl} mice, CPT1^{fl/fl}Lyz2^{cre} mice and CPT1^{fl/fl}TREM2^{fl/fl}Lyz2^{cre} mice were respectively identified by PCR.

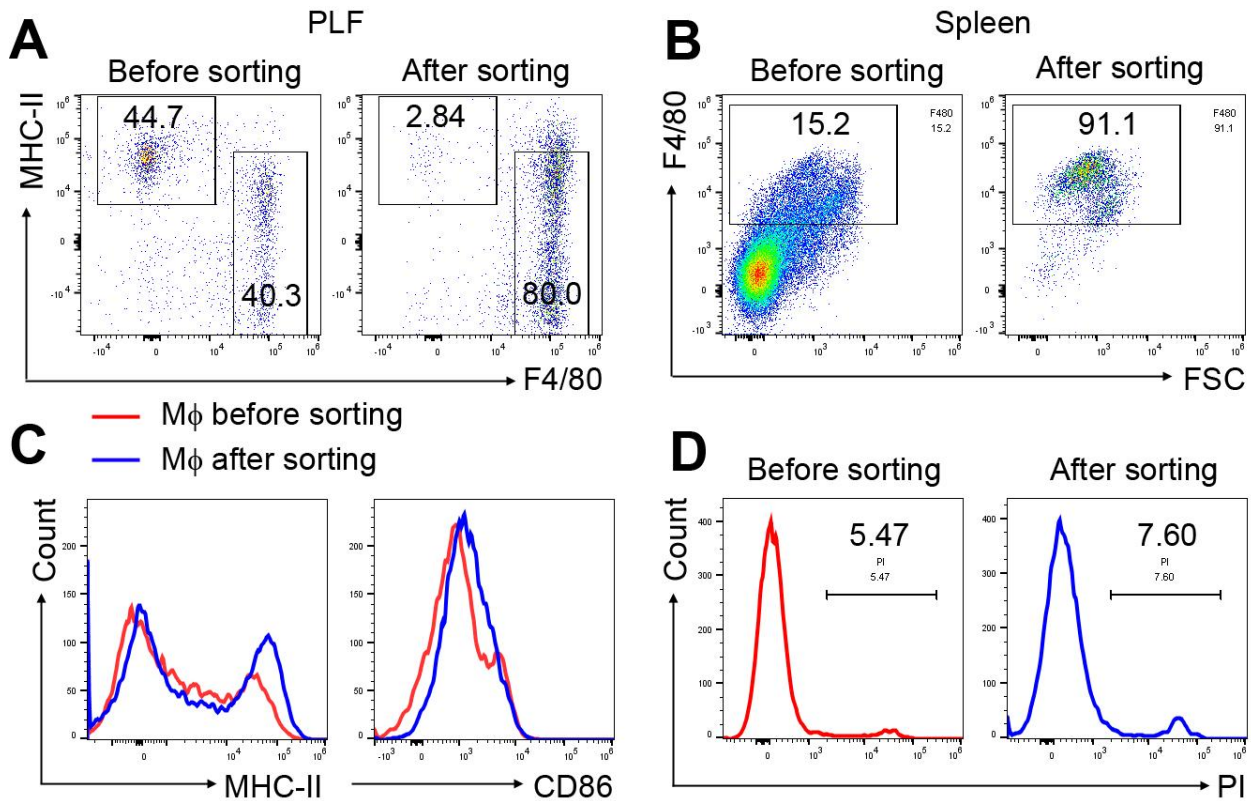


Figure S19. The purity and activating status of sorted cells. (A, B) Mouse macrophages (M ϕ) were sorted from PLF or spleen by positive selection using the magnetic cell sorting system. **(A)** The purity of peritoneal macrophages (mainly LPM ϕ , gated as CD11b⁺ F4/80^{high} MHC-II^{low} cells) was determined by flow cytometry before and after sorting. **(B)** The purity of splenic F4/80⁺ macrophages was analyzed before and after sorting. **(C)** The expressions of MHC-II and CD86 on splenic macrophages (gated CD11b⁺F4/80⁺) were detected before and after sorting. **(D)** The apoptosis (PI⁺) of splenic macrophages (gate CD11b⁺F4/80⁺) was detected before and after sorting.

Table S1. The characteristics of healthy controls and sepsis patients

Variables	Healthy controls	Sepsis Patients
Sample size (no.)	45	54
Sex-no. (%)		
Male	26 (57.8)	33 (61.1)
Female	19 (42.2)	21 (38.9)
Age (years)		
Mean \pm SD	50.93 \pm 17.07	59.37 \pm 21.83
Median (IQR)	55.0 (35.5, 66.5)	58.0 (45.5, 81.0)
Range	17-79	17-94
Blood parameters		
Hemoglobin (g/L)	132.0 \pm 7.22	111.4 \pm 21.86
Platelets ($\times 10^9$ /L)	249.1 \pm 37.35	125.1 \pm 71.38
White blood cell ($\times 10^9$ /L)	8.63 \pm 1.11	17.44 \pm 10.74
White blood cell (%)		
Neutrophil	59.6 \pm 3.968	86.96 \pm 7.033
Monocyte	5.922 \pm 0.987	4.813 \pm 2.827
Lymphocyte	32.98 \pm 3.162	7.249 \pm 6.054
Eosinophil	1.729 \pm 0.789	0.2574 \pm 0.4577
Basophil	0.4444 \pm 0.2062	0.2407 \pm 0.3288
Serum biochemical indexes		
Total Bilirubin (μ mol/L)	10.04 \pm 3.415	39.16 \pm 30.70

CRP (mg/L)	0.92 ± 0.569	100.9 ± 58.48
ALT (U/L)	23.24 ± 7.113	89.41 ± 75.70
BUN (mmol/L)	4.96 ± 0.735	15.43 ± 11.75
Glucose (mmol/L)	4.96 ± 0.511	8.962 ± 3.870
Triglyceride (mmol/L)	0.95 ± 0.304	2.326 ± 1.579

Abbreviations: CRP, C-reactive protein; ALT, alanine aminotransferase; BUN, Blood Urea Nitrogen.

All data are shown as Mean ± SD.

Table S2. Clinical Information of sepsis patients.

#	Gender	Age	Days in Hospital	Days in ICU	SOFA Score	Site of Infection	Outcome
1	M	84	19	8	10	Pneumonia, urinary tract infection	Survival
2	M	62	8	6	3	Pneumonia	Survival
3	F	66	12	5	5	Urinary tract infection	Survival
4	M	66	4	2	3	Peritonitis, cholecystitis	Death
5	M	71	14	2	2	Pneumonia	Death
6	F	83	11	6	2	Pneumonia	Survival
7	F	89	18	4	6	Pneumonia, bloodstream infection	Survival
8	M	55	59	31	8	Pneumonia	Survival
9	F	26	8	3	2	cholecystitis, pancreatitis	Survival
10	M	84	12	5	3	cholecystitis	Survival
11	F	69	21	4	3	Urinary tract infection	Survival

12	F	28	5	5	11	Bloodstream infection	Death
13	F	41	12	4	2	Peritonitis	Survival
14	M	54	11	2	9	Bloodstream infection, gastroenteritis	Survival
15	M	75	9	4	8	cholecystitis	Survival
16	F	94	23	23	15	Pneumonia	Death
17	M	88	15	8	9	Pneumonia	Death
18	M	22	57	13	10	Pneumonia, pyothorax, bloodstream infection	Survival
19	M	44	19	10	11	Pneumonia	Survival
20	M	56	18	18	13	Peritonitis, pneumonia	Survival
21	M	56	28	10	5	Meningitis, bloodstream infection	Survival
22	F	32	15	9	11	Pneumonia	Survival
23	M	35	18	11	8	Endocarditis, pneumonia, urinary	Survival

						tract infection	
						Pneumonia,	
24	M	55	2	2	15	bloodstream	Death
						infection	
						Biliary tract	
						infection,	
25	M	67	7	5	2	bloodstream	Survival
						infection	
						biliary tract	
						infection,	
26	M	85	14	5	3	bloodstream	Survival
						infection	
						Cholangitis,	
						pneumonia,	
27	M	59	18	7	12	bloodstream	Survival
						infection	
						Bloodstream	
28	M	70	38	3	4	infection	Survival
						Appendicitis,	
29	M	27	5	4	2	Peritonitis	Survival
						Pneumonia,	
30	F	88	17	5	3	bloodstream	Survival

						infection	
31	M	55	7	2	2	Pneumonia	Survival
32	M	47	13	9	8	Peritonitis	Survival
33	M	50	13	13	16	Bloodstream infection	Death
34	F	88	12	8	12	Pneumonia	Death
35	M	87	14	3	10	Peritonitis, cholecystitis	Survival
36	M	53	57	24	14	Pneumonia	Death
37	F	89	18	7	2	Nephritis	Survival
38	M	57	20	6	4	Bloodstream infection	Survival
39	F	74	23	1	11	Peritonitis	Survival
40	F	55	20	15	15	Pneumonia, ARDS	Death
41	F	79	17	17	5	Pneumonia, urinary tract infection	Death
42	M	36	21	5	6	Pneumonia	Survival
43	F	81	4	4	17	Pneumonia, ARDS	Death
44	M	46	25	1	8	Pneumonia, ARDS	Survival
45	F	62	5	5	8	Pneumonia, ARDS	Death
46	M	19	3	3	9	Pneumonia, Bloodstream	Death

						infection	
47	F	81	8	1	9	Pneumonia	Death
48	M	50	43	6	5	Pneumonia	Survival
						Pneumonia,	
49	F	83	3	3	14	bloodstream	Death
						infection	
50	M	20	12	6	8	Pneumonia	Survival
						Pneumonia,	
51	M	28	30	11	14	bloodstream	Survival
						infection	
52	M	68	9	9	9	Pneumonia	Death
						Pneumonia,	
						peritonitis,	
53	F	50	30	21	10	Bloodstream	Survival
						infection	
						Pneumonia,	
54	F	17	20	20	10	peritonitis	Survival

Table S3. Infection classification of sepsis patients.

Type of infections	Sample numbers
Bacterial infection	35
<i>Escherichia coli</i>	11 (20.4)
<i>Klebsiella pneumoniae</i>	10 (18.5)
<i>Acinetobacter baumannii</i>	5 (9.3)
<i>Staphylococcus</i>	5 (9.3)
<i>Pseudomonas aeruginosa</i>	4 (7.4)
Viral infection	3
<i>Influenza virus</i>	1 (1.9)
<i>Epstein-barr virus</i>	1 (1.9)
<i>Adenovirus</i>	1 (1.9)
Fungal infection	4
<i>Candida parapsilosis</i>	1 (1.9)
<i>Candida tropicalis</i>	1 (1.9)
Uncertain	2 (3.8)
Undefined*	12

*Undefined represents no clear microbe in pathogenic culture assays.